AIAA Propulsion and Energy Forum
19-22 August 2019, Indianapolis, IN
AIAA Propulsion and Energy 2019 Forum

10.2514/6.2019-4149

A Design for a Two-Stage Solid Mars Ascent Vehicle

Andrew Prince[1], Timothy Kibbey[2]
NASA Marshall Space Flight Center (MSFC), Huntsville, AL 35812, United States of America

Ashley Karp[3]
Jet Propulsion Laboratory (JPL), California Institute of Technology, Pasadena, CA 91109, United States of America

Abstract

A solid propulsion system design is being considered for a conceptual Mars Ascent Vehicle (MAV) as part of a potential robotic Mars Sample Return campaign. A Preliminary Architecture Assessment for a MAV is being conducted at Marshall Space Flight Center. Experts from all relevant areas are involved in a rapid design and analysis cycle to define a MAV vehicle utilizing solid propulsion. The design presented here is the solid motor propulsion concept result of the study. Whereas solid motors have been used on Mars missions in the past during descent, none have been required to reside on the surface for a period of time prior to functioning. This difference will expose the MAV to relatively extreme temperatures. Other challenges exist in designing a solid propulsion system for MAV including performance interactions with other vehicle inert masses and minimizing orbit dispersions. These considerations were examined and a preliminary CAD model of the motors was created. Along with additional pertinent inputs from other disciplines, a solid propulsion vehicle concept for the MAV is described.

I. Nomenclature

Burnout Q	= motor burnout dynamic pressure
I_{sp}	= specific impulse
Max Q	= maximum dynamic pressure
ΔV	= change in velocity

[1] Propulsion Lead, Solid Propulsion NASA MSFC, AIAA Senior Member.
[2] Senior Solid Propulsion Engineer, Jacobs/ NASA MSFC, and AIAA Member.
[3] Technologist, Propulsion and Fluid Flight Systems, Jet Propulsion Laboratory, California Institute of Technology, AIAA Senior member.

II. Introduction

The Mars Ascent Vehicle (MAV), as part of a potential Mars Sample Retrieval (MSR) campaign, is intended to transport samples from the Mars surface to an orbiting Earth return vehicle. MSR is envisioned as utilizing a series of three Earth launches. The first launch consists of a rover that collects Mars rock samples and deposits them for future recovery (Mars 2020). The second and third launches, potentially as early as 2026, would deliver the MAV as part of a Sample Retrieval Lander (SRL) and the Earth Return Orbiter (ERO). The MAV would descend to the Mars surface onboard the lander. The SRL would retrieve the samples and insert them into the MAV before returning to the ERO and Earth. An overview of the Mars Sample Return Campaign is shown in Fig. 1.

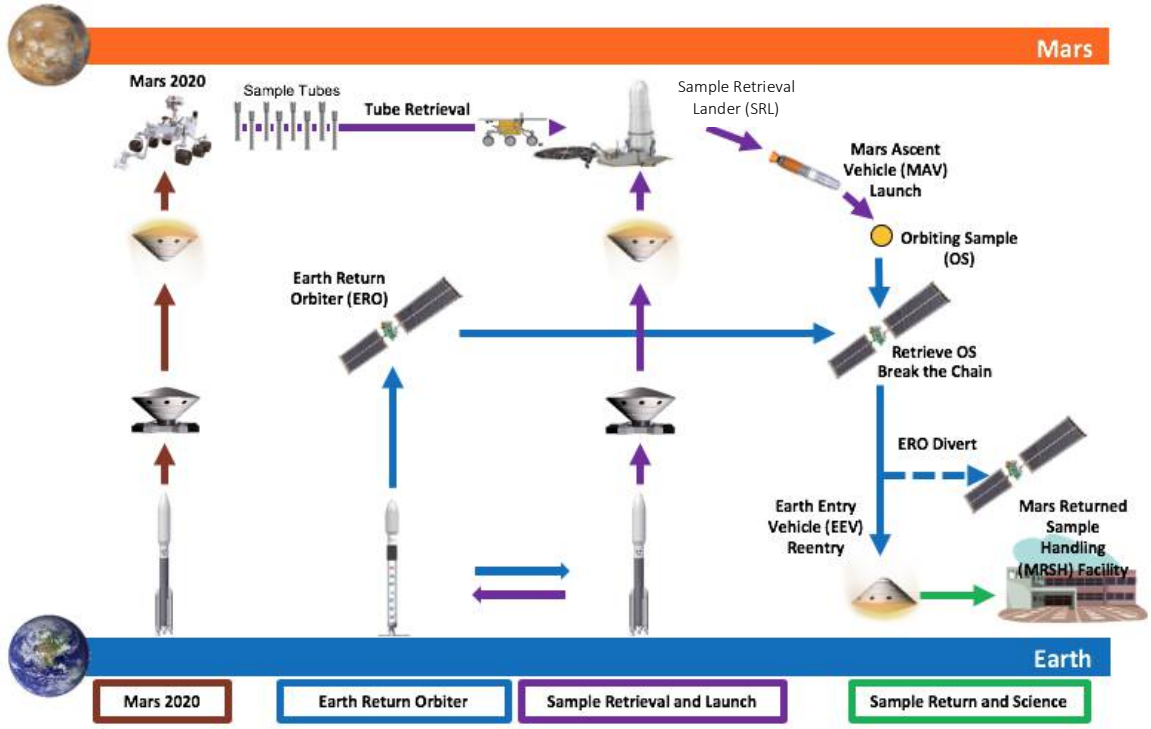

Fig. 1 Mars Sample Return Campaign.

The MAV is particularly influential to the overall MSR mission architecture because it helps set performance requirements for the lander and Earth Return System. Of particular interest is the MAV propulsion system and its associated trades. This paper describes the current development of a two-stage solid motor MAV and the various research that has shaped the project.

III. MAV Mission Solid Option

Consideration of a MAV vehicle has been ongoing for many years through different efforts. Configurations have changed with various propulsion systems considered. Since 1998, the derived solutions have been minimum mass solid propulsion solutions as shown in Fig. 2.

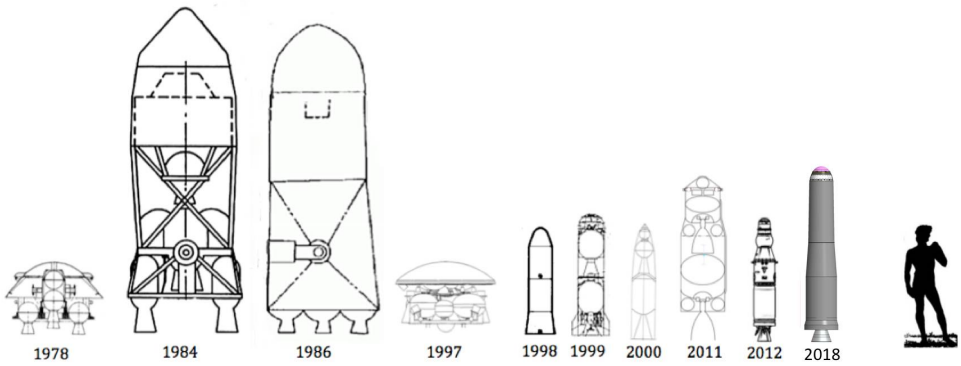

Fig. 2 MAV concept history.

A two-stage solid rocket motor MAV has been studied in the past [1], however, low-temperature requirements made the option much more challenging. The current design calls for housing the MAV in the SRL, which would be responsible for delivering the MAV to Mars, maintaining its thermal requirements, and launching it. The SRL is expected to keep the MAV between -40 °C and +40 °C, enabling the use of propellant that has already been qualified for that temperature range. Prior to MAV operation, the SRL would raise the temperature of the MAV to -20°C. The current MAV design consists of two solid rocket stages built around a low-temperature-capable propellant (Fig. 3).

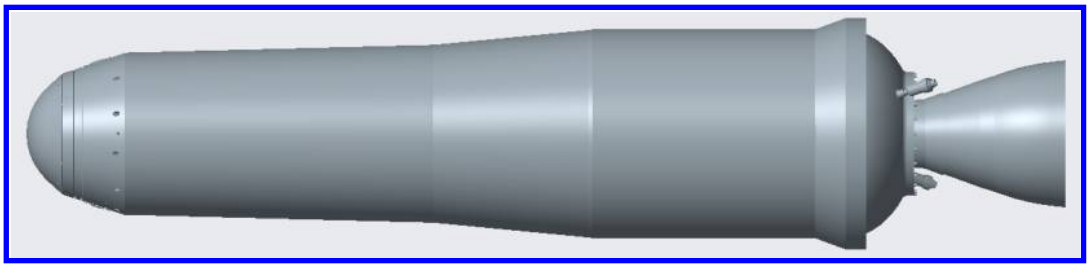

Fig. 3 Concept drawing of a two-stage solid MAV.

The mission design is moving through architecture space as a balance between systems in capability, schedule, and resources is determined. As a result, firm requirements have not been established. In lieu of requirements, Ground Rules and Assumptions (GR&A) have been used [2] and are listed in Table 1.

Table 1 Ground Rules and Assumptions.

Property	Value	Comments
Minimum Orbit Altitude	300 km	JPL Defined
Eccentricity	0.006	
Semimajor Axis	+/- 9 km	
Target Orbital Insertion Inclination Angle	25° (Trade Space 18° to 25°)	
GLOM Target	400 kg	
Launch Altitude	-2.5 km	
Max Angle of Attack	4°	
Max Vehicle Length	2.80 m	
Max Vehicle Diameter	.57 m	
Quasi Static Load	Lateral 15g	
Operational Temp	-20°C +/- 2°C	
Non-Operation Temp	-40°C to +40°C	
Prop System Qualification Temp (wetted)	Non-Operation +10 / - 10 C	
Prop System Qualification Temp (non-wetted)	Non-Operation +20 / -15 C	
Launch Angle	30-60°	
MPA (20 Sample tubes)	16 kg	
Structural Safety Factor	1.25	
Max Nozzle Vector Angle	5°	6 DOF Based
Bondline Temperature Limits	93°C	MSFC Defined

IV. Design Methodology

With the GR&A as constraints, motors for each stage and solution could be sized using trajectory analysis provided by the Guidance Navigation and Control (GNC) group. GNC provided thrust shape and propellant mass required for the desired ΔV for each stage. The motor grain, case, and nozzle could then determine a grain shape and nozzle design to meet the GNC recommendations. This could be fed back to the GNC for trajectory analysis to close the design loop. By the time of this paper, this loop has been completed twice, with numerous refinements of both motor design and the GNC design also being made in parallel.

Thermal and structural analysis of the propellant grain, case, and nozzle have been performed and proved important in not only setting the matured design but understanding the sensitivities and trades upon which the design process focused.

A. Initial Sizing

The preliminary trajectory for the two-stage solid MAV concept is like two nearly impulsive (instantaneous) burns separated by a long coast (Fig. 4). Stage 1 (ST1) puts the vehicle into a highly elliptical orbit with an apoapsis at the desired altitude of the circular orbit, but with a negative periapsis. Once the vehicle has coasted up to nearly apogee, Stage 2 (ST2) fires to circularize the orbit.

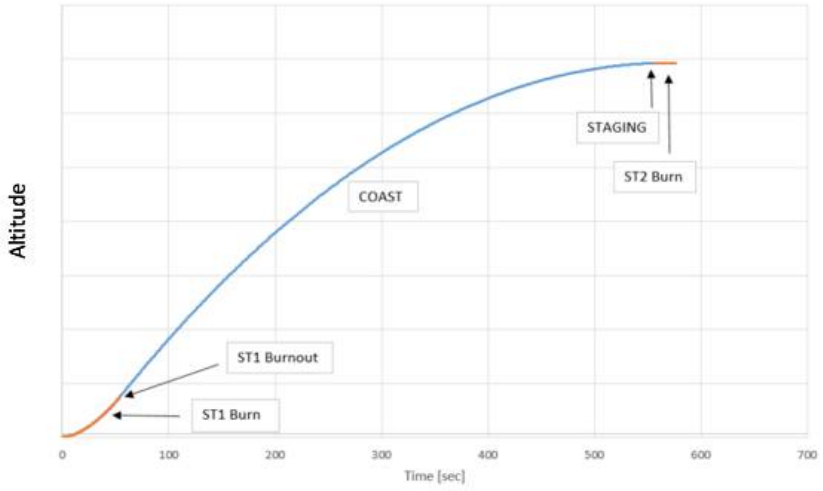

Fig. 4 MAV trajectory.

Both stages have affinity with demonstrated in-space motors and have thrust vector controlled (TVC) nozzles. The first stage has some peculiarities driven by vehicle performance needs; it must burn longer than a typical motor of its size. The need for this showed up in two ways. First, the trajectory analysis included a thrust optimization scheme subject to specific physical constraints. This routine recommended initial thrust at the maximum possible (boost) and a reduced thrust extending the burntime to 55 s. Secondly, the reaction control system (RCS) is designed to maintain attitude after the first-stage motor burns out. Sensitivities to this will be discussed below.

B. MAV Idiosyncrasies

The small payload and stage sizes drove unconventional sizing interactions. Figure 5 a) shows a representative larger stage. Most of the stage's inert mass is driven by the propulsion choices. Because of this propulsion and the other systems are designed separately. Conversely, the MAV second stage non-propulsion inert mass (Fig. 5 b) is approximately 75% of the mass (excluding payload). This is due to the avionics, RCS, thermal control systems, and the structure necessary to house and connect them to the payload and inter-stage structure. This causes MAV performance optimization to be more linked across systems.

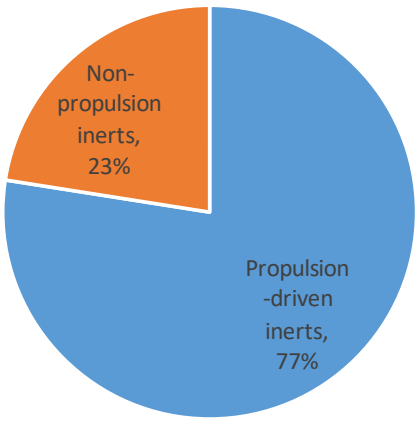

a) Sample large-stage mass proportions.

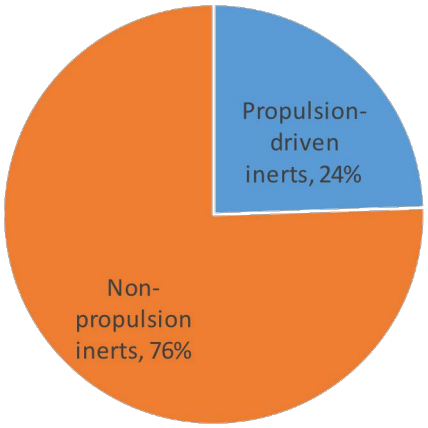

b) MAV small-stage proportions.

Fig. 5 Propulsion inert masses of representative stage and MAV Stage 2.

At the beginning of the Preliminary Architecture Assessment (PAA), limits to this historic approach led to a recognition of the non-propulsion components needing to pay closer attention than normal to mass and volume. But the development process identified additional key interactions between systems.

The RCS must conduct control maneuvers during a long coast between stages. RCS can be strongly taxed right at ST1 burnout if the aerodynamic forces are significant. A longer first-stage burntime results in a lower dynamic pressure at burnout reducing the disturbances RCS must counteract (Fig. 6). It was estimated that 65 s was long enough to keep RCS propellant at a tolerable level and thus set as nominal. Figure 7 shows this and similarly sized commercial motors.

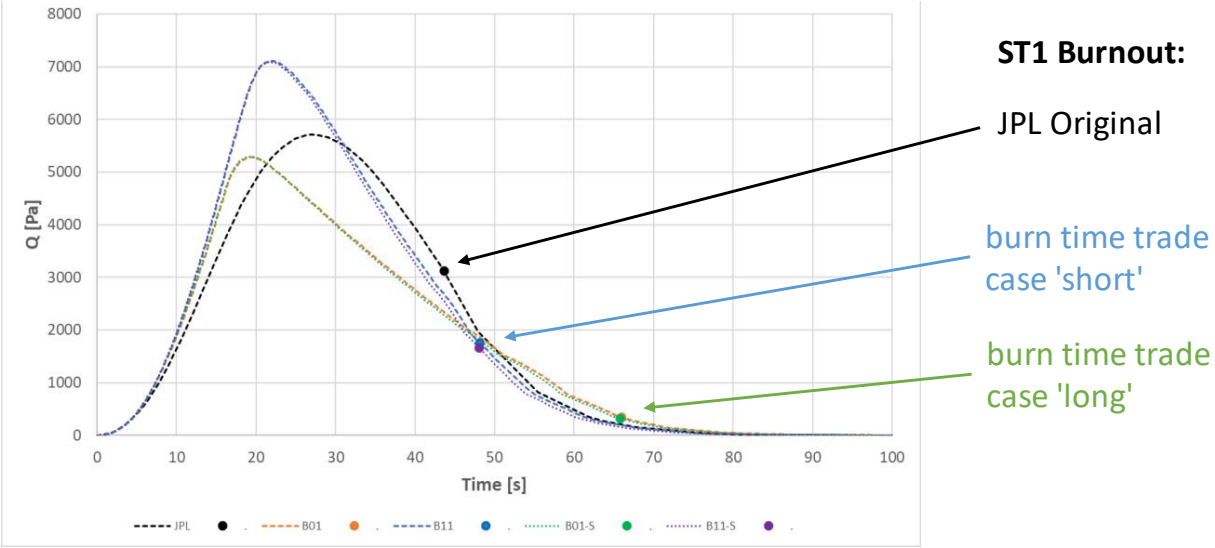

Fig. 6 Example dynamic pressure.

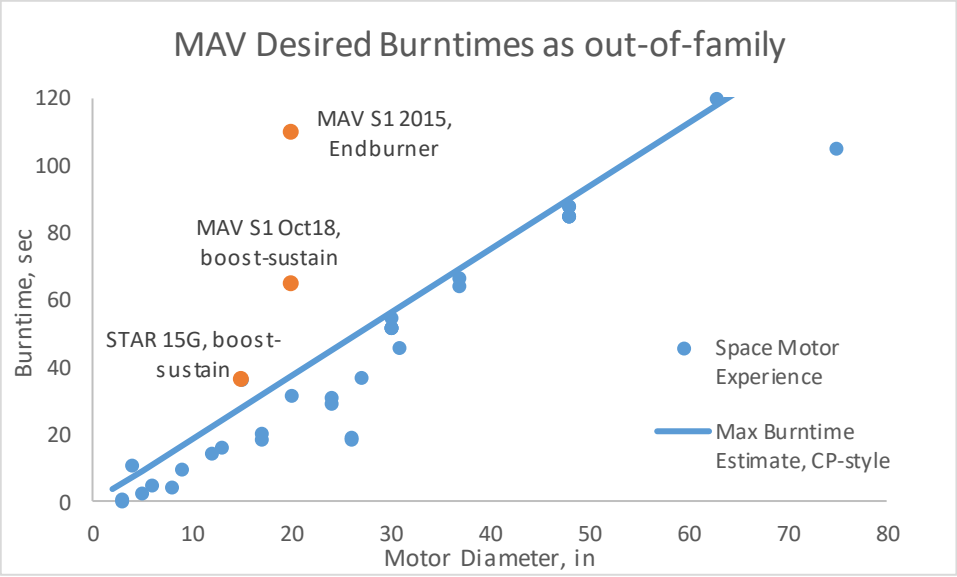

Fig. 7 Space motor experience for burntime with diameter.

Furthermore, RCS sizing estimates suggested that the "short" first-stage burntimes could increase the RCS propellant loading, volume, and associated structure by 10 kg or more. Trajectory work also showed that second-stage mass affects gross liftoff mass (GLOM) twice as much as first-stage mass for a paired design set. Therefore, solid

rocket motor 1 (SRM1) inert mass increases as high as 20 kg or more would be an appropriate price to pay to limit dynamic pressure at burnout.

In the second-stage, variations are assumed to compound affecting the final orbit. GNC and propulsion teams each performed trade studies and found that impulse-conserving burntime variation, due to propellant burn rate, caused very little variation in orbit. However, I_{sp} variation of the upper stage led to a variation of tens of km in apoapsis or periapsis altitude. This led to an increase in the target orbit in order to keep any lower-performing vehicles above 300 km periapsis.

C. Propellant Mass Fraction Estimation

Mass correlations for the first stage must allow for the motor to have a higher inert mass fraction than typical for motors of this size. More of the insulation gets exposed early in burn, and as a result, both the insulation and the nozzle phenolics are exposed for longer, thus they must be thicker. For the second stage, no similar constraints were found, so it is very much in line with similar commercial 17-inch motors, just with the addition of TVC.

Non-dimensional relationships can provide both convenience and instruction [3]. One way to communicate the relationship between propellant and inert masses of a motor is the Propellant Mass Fraction (pmf), which is the ratio of propellant mass to total motor mass. This is distinct from stage inert mass, because it does not include auxiliary hardware such as RCS, avionics, separation systems, etc., whose masses are not related directly to motor size. A previous paper on this MAV concept [4] showed correlations of mass fraction as a function of mass to predict motor masses at the concept phase. These are repeated in Fig. 8 along with the points demonstrating development progress during this study. Preliminary estimates were optimistic prior to accounting for the relationships discussed above. The vehicle was sized then ballistic design and initial CAD were performed. The initial pmf was lower than typical until a series of optimizations and trades were performed, which matured the CAD predicted masses and raised the pmf closer to predicted values.

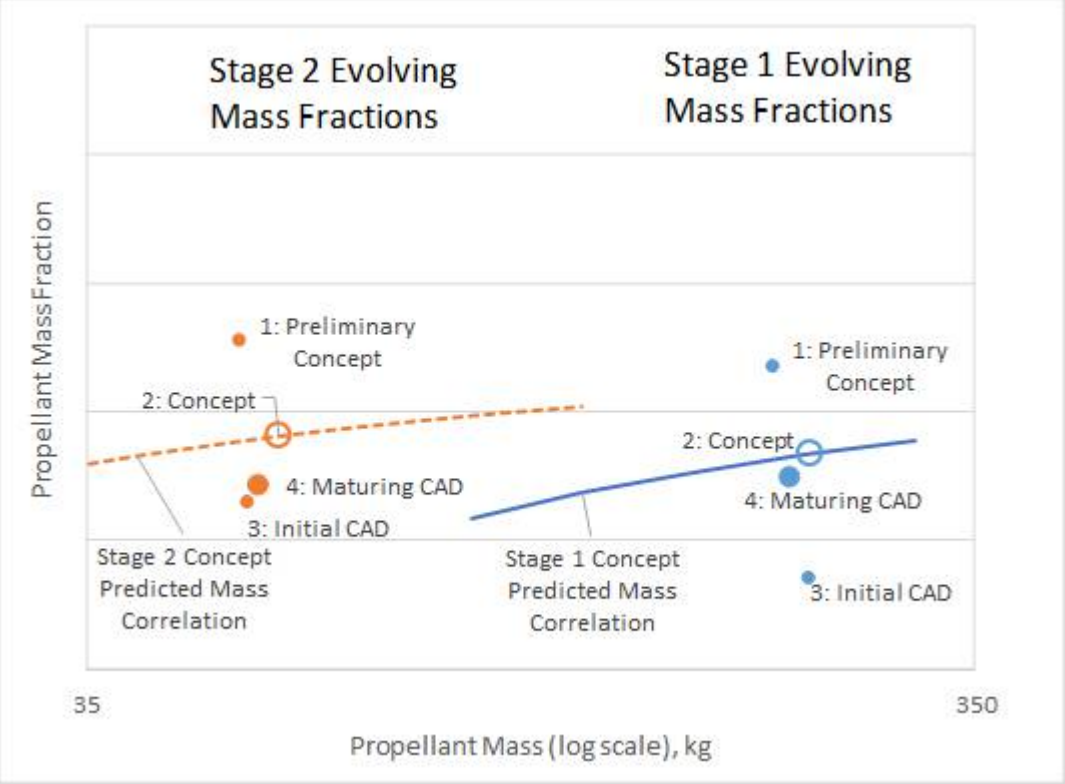

Fig. 8 Evolution of MAV propellant mass fraction.

The full evolution of propulsion to vehicle mass is shown in Fig. 9. For Stage 1, preliminary showed that the motor case assumption for titanium at high operating pressures was not consistent with the initial mass estimate. The preliminary CAD was further refined to when the team optimized ballistics and switched to a composite case. This

included an optimization of internal ballistics designs that was able to reduce insulation mass and a trade on operating pressure and nozzle throat area. On the Stage 2 plot, the concept advanced by considering a refined nozzle design offset by nozzle length. On the GLOM plot, the team reduced the payload requirement and margin as the payload design matured; this offset the other mass increases to keep the GLOM from having to grow significantly. Note the maturing CAD-based masses for Stage 1 and Stage 2 are very close to the concept masses, respectively, thus defending the concept as a useful model.

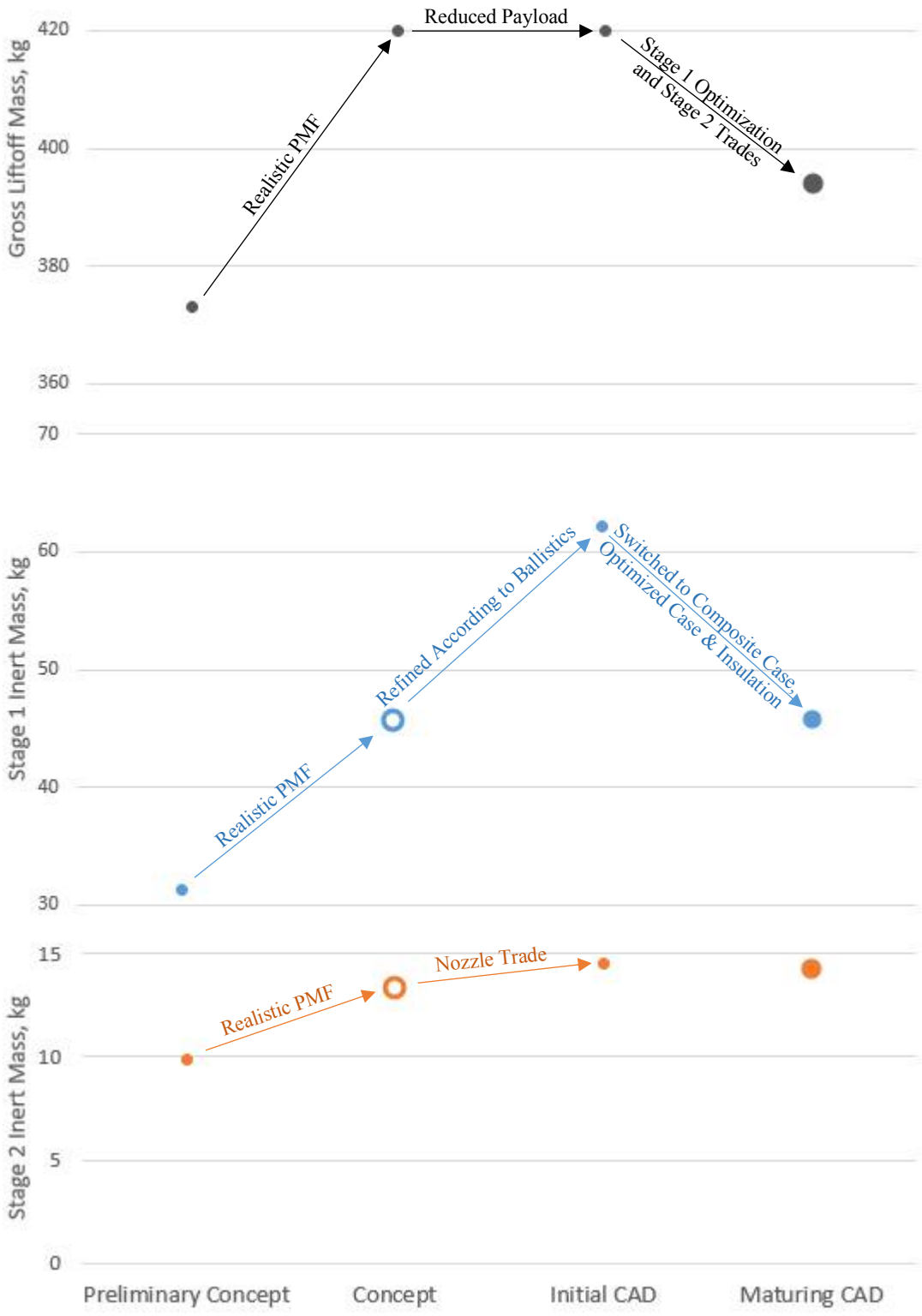

Fig. 9 Propulsion and vehicle mass evolution summary.

V. Optimization Trades

A. Nozzle Length/Mass vs. I_{sp}

Once the motor designs progressed to the initial CAD phase, opportunities were sought to reduce mass and length while increasing vehicle performance. The second-stage nozzle led to increased performance by trading I_{sp} for nozzle length. The reference motor at this point assumed a nozzle expansion ratio of 81 and an I_{sp} of 293 s. The initial CAD showed that truncating the nozzle would save about 7 kg per meter (or 0.4 lbm per inch). More importantly, the structure assumption used for the inter-stage skin (1/8-inch thick aluminum) led to an even stronger mass savings available, about 13 kg per meter (or 0.7 lbm per inch). Partial derivatives from trajectory analysis were used to estimate a series of vehicle performance values as a function of nozzle and inter-stage length. This led to a convergence point that provided a significantly shorter inter-stage and nozzle (Fig. 10) and predicted mass savings, despite an I_{sp} reduction, of approximately 10 s. Furthermore, this study encouraged a decision to move the separation plane closer to the Stage 2 motor, made easier by the shortness of the nozzle.

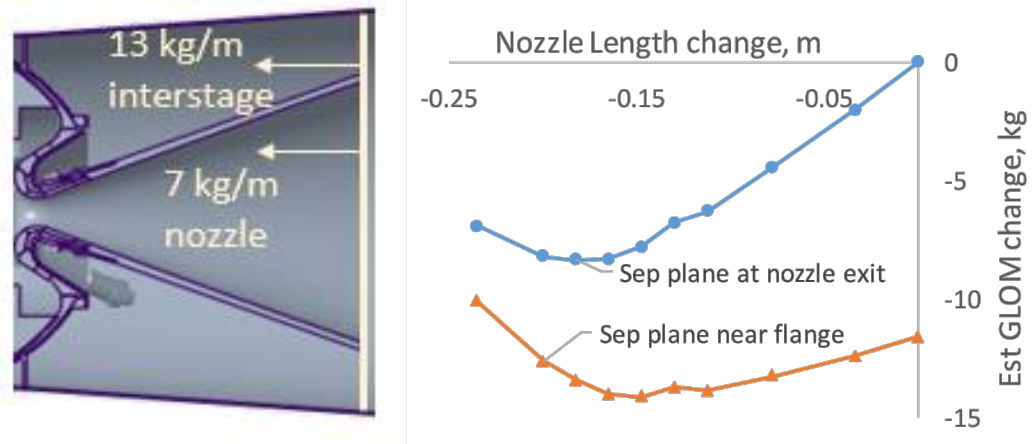

Fig. 10 Optimization of nozzle length.

B. Guided System vs. Unguided

Unguided, spin-stabilized rockets are common for applications where mass is at a premium and orbital accuracy is not as important. For the MAV design, an unguided system would reduce the mass of the RCS and accompanying structure. However, in this case a spin-stabilized, unguided upper stage increased orbital variations to about 300 km. In order to maintain this mission's minimum periapsis requirement of 300 km, the target orbit would have to be increased significantly. This increased energy requirements, which in turn caused propulsion masses to increase, offsetting any gains from RCS reduction. For these reasons, the unguided system was abandoned for the MAV mission.

C. Metallic Stage 1 vs. Composite Case

An initial concept mass fraction correlation was developed by comparing boost-sustain composite-case motors [5] of the same size. Furthermore, it had a high maximum operating pressure (MOP) near 1500 psi. These assumptions were used during the initial CAD work until this showed that a titanium case would be significantly heavier than expected. Designs for both a composite case and titanium case were brought forward, at both 1500 psi and 1000 psi MOP. The lower pressure was realized by increasing the nozzle throat diameter at the same nozzle exit size. Once again I_{sp} was being traded for mass reduction. A minor 4–5 s I_{sp} reduction resulted from the throat increase due to nozzle length and exit area ratio changes. Insulation mass scales with pressure so in addition to the case, insulation mass savings were captured. Based on these findings, the team selected a composite case motor with a 1000 psi MOP, enabling significant GLOM savings.

D. Stage 1 Length, Diameter, and Aero Ramp vs. Stability

As discussed above, the early performance studies assumed a 65 s burntime in order to limit dynamic pressure at burnout. A preliminary 6 Degree of Freedom (DoF) analysis showed a reasonable amount of RCS propellant was

required. Stability sensitivity was investigated in moving the center of gravity aft by 0.1 and 0.2 m. This variation represents the uncertainty in the aerodynamic model as well as future possible design changes. It was found that a 0.2 m change would greatly increase the RCS propellant required to retain a stable angle of attack until the vehicle had coasted long enough for dynamic pressure to become negligible. In order to increase the robustness of the design or possibly reduce max RCS usage, two choices were investigated:

1) Increase the size and effectiveness of the aft aerodynamic surface by reducing the first-stage motor diameter.
2) Further extend the burntime of the first-stage motor to reduce burnout dynamic pressure.

A set of motor design trades was conducted to investigate these choices. Reducing the first-stage diameter presented a complication. The smaller the diameter, the harder it is to maintain a significant thrust level during the sustain portion of burn, because the motor is acting as an end-burner at this time. Compounding this, the MOP reduction from the composite case trade increased the burntime about 10%. This made lengthening the first stage unattractive. Therefore, the initial motor diameter was maintained and burntimes of 72 s or longer targeted.

Updated trajectory analysis showed that 72 s of burntime reduced the dynamic pressure to one third of the value of the 65 s trajectory. The 6 DoF analysis also showed that the required RCS propellant was reduced by 32%.

VI. Motor Development Refinements

A. Reaction Control System and Stability

RCS will provide roll control of the MAV vehicle during the Stage 1 powered flight (Fig. 4). At first-stage burnout, the vehicle coasts. While coasting, RCS will control all three angular DoF, stabilizing the vehicle until second-stage initiation. RCS will again control roll during Stage 2 burn and may be used to perform vehicle separation or deorbit maneuverers not yet defined.

B. Motor Grain Optimization

Preliminary CAD grain design focused on matching the boost-sustain thrust trace provided by the GNC initial trajectory assessment. Optimization was needed to reduce inert mass and length.

A handful of geometric parameters that controlled the pressure and thrust trace and insulation exposure times were examined. Also, a set of constraints such as burntime and fraction of impulse in the "boost" phase was levied to limit solutions to the desired class of thrust traces. The Solid Performance Program (SPP)[20] code was used over a design space of these variables, then a surrogate model and optimization techniques were used to predict optimum grain designs. Initially, minimum length was selected as an optimizing variable, but this is not the main driver of performance. Length also appeared to incentivize large throat diameters that might overly reduce I_{sp}. Based on these observations, an estimate of stage ΔV given a constant upper stage was derived. This included the effects of insulation and case mass as well as nozzle I_{sp}.

The results of this optimization are shown in Fig. 11 for three different propellant mass targets. The optimization was able to reduce motor chamber length by about 4 inches and reduce insulation mass by about 10 pounds. Additional details of this effort are to be shared in an upcoming AIAA forum by R. Hetterich.

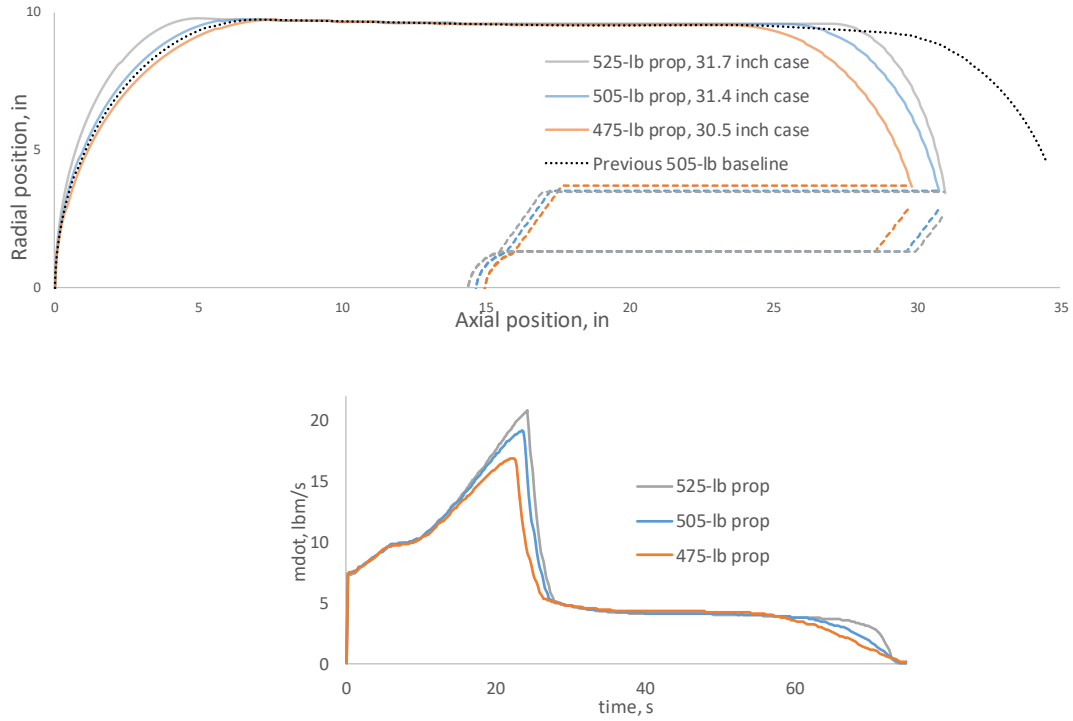

Fig. 11 Motor grain optimization.

C. Trajectory Design of Experiment

As shown in the above designs, interaction of subsystems and components other than propulsion is capable of driving the MAV vehicle and propulsion system designs. It is beneficial to characterize a broader design space of potential vehicle masses as well as propulsion masses. Leveraging this idea, a Design of Experiments (DOE) was conducted to guide final motor design selection of both stages.

The goal of the DOE was to link Stage 1 and Stage 2 vehicle inert mass ranges to propulsion design ranges. A 12-run matrix was developed considering the following three Stage 1 variables:

1) SRM1 propellant mass – 3 levels, from the Motor Grain Optimization output
2) Stage 1 inert mass – 2 levels, a range of 14 kg to cover structural assumptions as well as the titanium or composite case trade
3) Stage 1 I_{sp} – 2 levels, representing a nominal or a 4-inch-extended nozzle

Stage 2 mass margin was computed for each of these cases, and if it was more than 5 kg, the Stage 2 motor was offloaded instead. Thus, the DOE predicted a Stage 1 motor propellant mass target given future updates of the masses of non-propulsion systems on either stage.

The results over this design space are shown in Fig. 12, highlighting the class of vehicle assumptions that accomplish the mission with less than 400 kg GLOM. Maturing the CAD showed that Stage 1 motor inert masses were very close to these low inert mass points. Trajectories delivered the expected ~4 kg payload margin. CAD progress also suggested Stage 2 non-propulsion inert mass was increasing. Interpolation within DOE was used to identify Stage 1 motor designs that limit the GLOM while accommodating these increases.

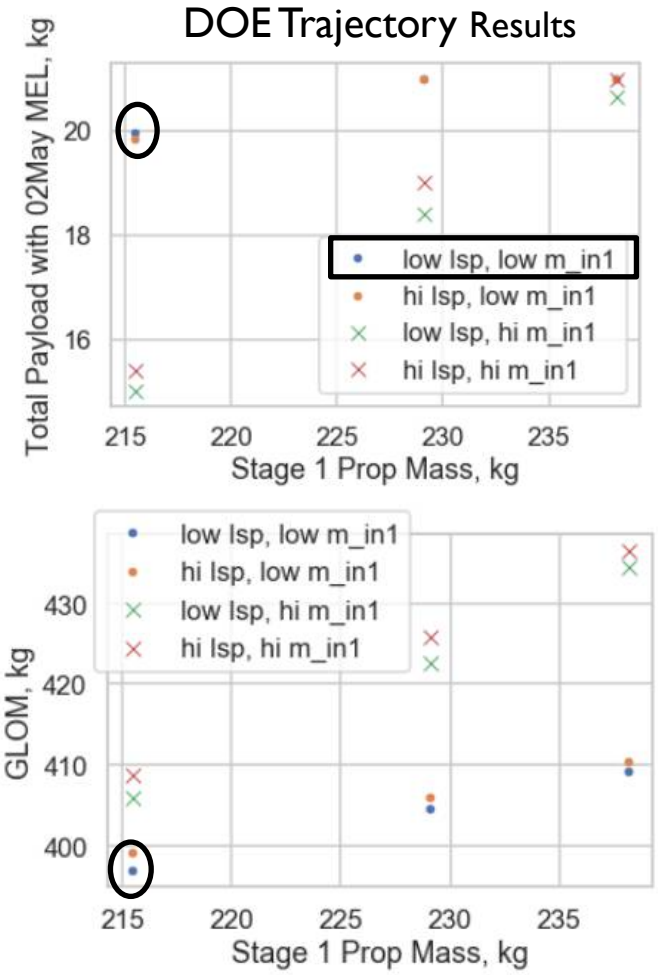

Fig. 12 DOE trajectory analysis.

VII. Risk Reduction Activities

Propellant selection was based on a number of factors such as low temperature capability and flight history [4]. The selected propellant has a Carboxyl-Terminated Polybutadiene binder and 86% solids. The same propellant was used on the Pathfinder and Mars Explorer Rover missions. However, this propellant had not been manufactured since 2002 and some ingredients faced obsolescence issues.

Challenges exist in designing the motors to utilize this propellant and meet structural margins. Current qualification minimum temperatures are -50 °C. Designing for propellant grain shrinkage and understanding the limitations are key.

An effort was undertaken to mitigate these risks by performing tensile and Propellant-Liner-Insulation tests. At the time these tests were planned, it was unknown if the MAV solid motors would be end burning or center perforated. Two analog sample types were developed to replicate each geometry. Insulated logs simulated an end-burning configuration (Fig. 13), while center-perforated representative samples were replicated by Strain Evaluation Cylinders (SEC) (Fig. 14). Both types of samples were manufactured from the candidate propellant with various web fractions. Typically for a center-perforated grain configuration, higher web fractions, or a higher percentage of the radius from the wall being propellant, increase thermal strain and the possibility of cracking. These analog samples were subjected to increasing lower temperatures then periodically x-rayed for anomalies and measured to determine actual strain.

Fig. 13 End-burning "insulated log" analog samples.

Fig. 14 Center-perforated SEC analog samples.

Data from the analog samples showed cracking at approximately -70 °C. All of the analog SEC remaining samples cracked when subjected to a rapid thermal transient from approximately -70 °C to 40 °C. Some of the SEC samples showed bond failures near the ends, possibly due to manufacturing issues. From the data it can be theorized this provided some strain relief in the 70% web fraction samples. A key finding was the highest web fraction survived in excess of -70 °C.

These results are specific for this sample design. Analysis will be required to replicate the testing and apply it to the planned MAV motor designs, which are larger in diameter.

Simultaneously, a 17-inch motor, which is the same relative size as the MAV second stage, was cast with this propellant and will be fired after being conditioned to the planned operational temperature of -20 °C (Fig. 15). The test data will be used in structural analysis to design the propellant relief mechanisms for this proof of concept motor. This activity is a proof of concept intended to show that the selected propellant is capable of use on MAV. This activity is currently planned to occur late in the 2019 calendar year.

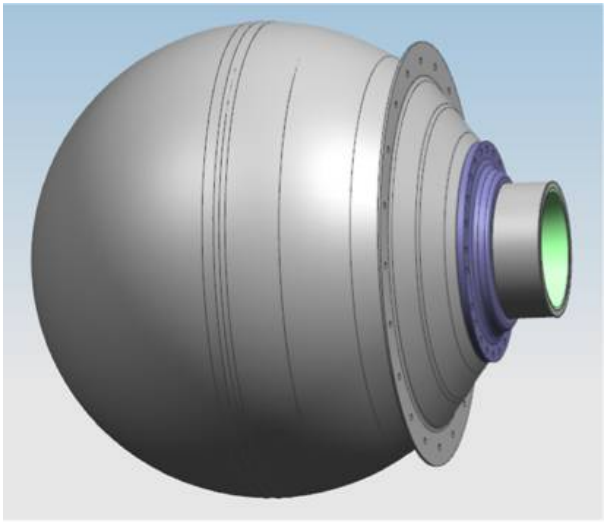

Fig. 15 Second-stage analog motor.

VIII. Conclusion

A conceptual design was completed of a two stage MAV solid propulsion vehicle shown in Fig. 16. Design of the motors occurred concurrently with other subsystems. An established set of ground rules and assumptions were targeted, with drivers including a GLOM of 400 kg, length of 2.8 m, maximum diameter of 0.57 m, and reaching an orbit of at least 300 km. Trades were investigated including GNC schemes, interactions with other vehicle structure masses, aerodynamics, and motor length. These optimizations culminated in a vehicle that met limits stated in the GR&A.

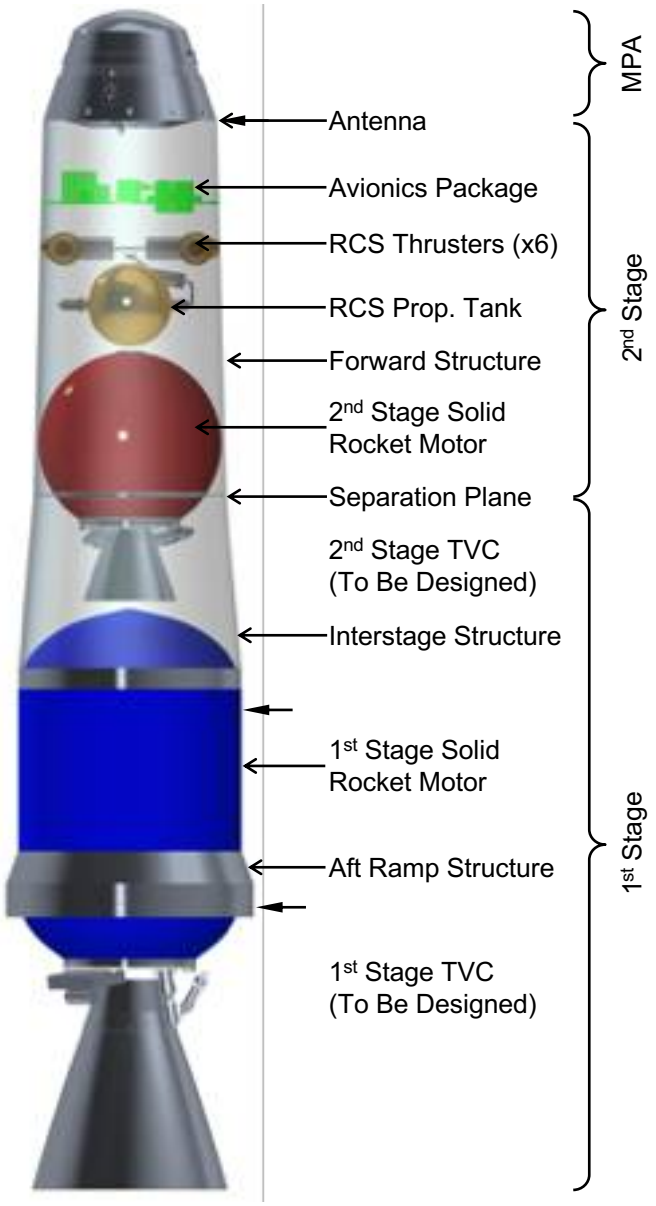

Fig. 16 MAV solid propulsion vehicle.

Given Stage 2 mass will drive vehicle GLOM, and length on the lander is at a premium, an initial study was made comparing orbital results of a guided and un-guided system. A guided system was shown to be superior with potentially a much lower semimajor axis and eccentricities.

While designing a guided first and second stage motor mass was minimized through material changes. Other interactions were also found to have the same result such an inter-stage affects, moving aero surfaces, burntime, and grain contours. The resulting designs fit well with sizing parameters of other commercially available systems suggesting manufacturability is reasonable (Fig. 17).

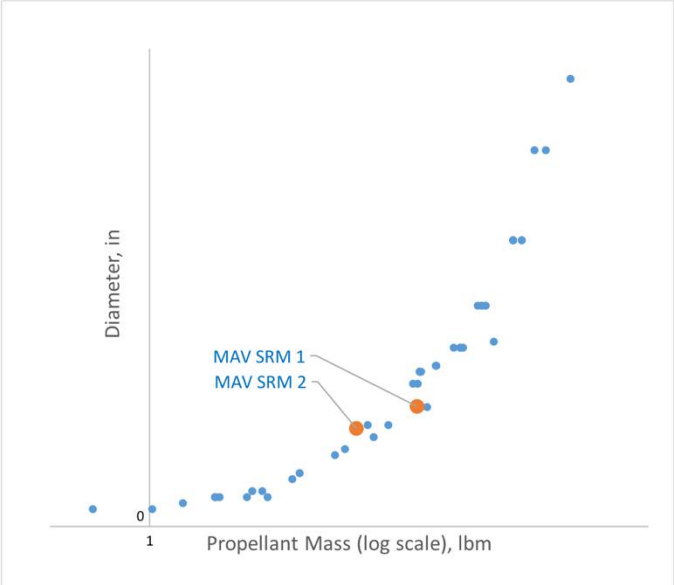

Fig. 17 MAV solid motors in family with commercial systems.

One of several potential propellants was selected as the basis for this study. The subject propellant does have a high TRL since it has been used in two other Mars landing programs as a Rocket Assist Deceleration motor. These have been fired nine times during Entry, Landing, and Descent into the Martian atmosphere. Experience for the environmental effect of dwelling on Mars prior to use was bolstered by testing analogs to the motors design. These were subjected to similar environments and could be used to further optimize the motor design features, such as stress relief flaps, in later design and analysis cycles.

Future work will include further design optimization as other vehicle subsystems mature. This includes reducing nozzle mass, fine tuning propellant mass based on other inter masses, and possible methods of reducing orbit dispersions. Reducing dispersions could be accomplished through a more complicated GNC-controlled energy management solution utilizing propellant margin reserves or by increasing RCS propellant load and implementing maneuvers post second-stage burn. While preliminary work has been completed, more detailed thermal and structural analysis review will take place as the MAV solid motors move forward.

Based on the described work, a MAV solid propulsion system was designed that allowed the vehicle to maintain a GLOM 6 kg below the 400 kg limit. The motor designs are flexible in that margins exist for on-loading propellant and minor geometry changes to motor length proving flexibility in GLOM and payload. GNC iterations will continue as the study progresses and the solid motor design will in-turn adjust within the evolving GR&A envelopes.

Acknowledgments

The authors would like to thank JPL for support and direction. They would also like to thank Angie Jackman and Shawn Skinner. The authors thank and appreciate the testing support provided by Northrup Grumman Innovation Systems located in Elkton, Maryland. Reference herein to any specific commercial product, process, or service by trade name, trademark, manufacturer, or otherwise, does not constitute or imply its endorsement by the United States Government or the Jet Propulsion Laboratory, California Institute of Technology.

References

[1] Shotwell, R.: "History of Mars Ascent Vehicle development over the last 20 years." IEEE Aerospace Conference 2016. DOI: 10.1109/AERO.2016.7500823.

[2] Farrington, A.: "Peer Review Overview and Objectives," internal presentation, 8 May 2018.

[3] Kibbey, T.P.: "Solid Rocket Motor Incremental Modeling for System Impacts," JANNAF/NASA MSFC In-Space Chemical Propulsion TIM, Huntsville, AL, August 2018.

[4] Prince, A.; McCauley, R.; Kibbey, T.; McCollum, L.; Oglesby, B.; Stefanski, P.; "Mars Ascent Vehicle Propulsion System Solid Motor Technology Plans," Conference Paper, IEEE Aerospace Conference (AeroConf 2019); Mar. 2019; Big Sky, MT; United States.

[5] Northrup Grumman Innovation Systems: "Propulsion Products Catalog, June 2018," OSR No. 16-S-1432. URL: https://www.northropgrumman.com/Capabilities/PropulsionSystems/Documents/NGIS_MotorCatalog.pdf, 15 March 2006 [retrieved 19 Nov 2018].
[6] Presentation, "MAV First Stage Design Kickoff Introduction", Scott Doudrick, 16 Jan 2014.
[7] "Mars Ascent Vehicle First Stage Development," 2016 JANNAF Space Propulsion Subcommittee Meeting, December 2016.
[8] Presentation, "MAV S1 Task Summary: Solid Challenges," Rachel McCauley, 27 Aug 2018.
[9] Presentation, "Peer Review Overview and Objectives", Allen Farrington, 8 May 2018.
[10] Kibbey, T. P., *Solid Rocket Motor Incremental Modeling for System Impacts,* JANNAF/NASA MSFC In-Space Chemical Propulsion TIM, Huntsville, AL, August 2018.
[11] Propulsion Products Catalog, Orbital ATK, Elkton, MD, October 2016.
[12] "American National Standard Mass Properties Control for Space Systems", ANSI/AIAA S-120A-201X.
[13] Office of Planetary Protection (2016, September 9th) – Retrieved from https://planetaryprotection.nasa.gov/overview.
[14] Treatment of Solid Rocket Motors That Complies with Established Protocols to Ensure Planetary Protection, Adrian Soler-Luna and Philip L. Stefanski, Jacobs ESSSA Group, Huntsville, Alabama, April 6, 2017.
[15] ESSSA-FY16-2947, Accelerated Aging with Respect to the Europa Braking Motor, Philip Stefanski, Huntsville, Alabama, September 21, 2016.
[16] Motor Age Life as Function of Bake Out for Bio-Reduction, Philip Franklin, NASA-Marshall Space Flight Center, Alabama, September 12, 2016.
[17] Advances in Sterilization and Decontamination – A Survey, NASA Contract NAS1-14209, The Bionetics Corporation, Hampton, Virginia, 1978.
[18] DOS Planetary Protection Approach, Pat Lampton and Sadie Boyle, NASA-Marshall Space Flight Center, Alabama, March 2017.
[19] Britt Oglesby, Andrew Prince, George Story, Ashley Karp, "Qualification of a Hybrid Propulsion System for the Mars Ascent Vehicle" 2019 IEEE Aerospace Conference, March 2019, paper #2126.
[20] Solid Propellant Rocket Motor Performance Prediction Computer Program (SPP), Sierra Engineering & Software, Inc.